Processing–Properties–Applications Relationship of Nanocomposites Based on Thermoplastic Corn Starch and Talc

Olivia V. López,[1] Luciana A. Castillo,[1] Silvia E. Barbosa,[1] Marcelo A. Villar,[1] M. Alejandra García[2]
[1]*Departamento de Ingeniería Química, PLAPIQUI (UNS-CONICET), Bahía Blanca, Argentina*

[2]*Centro de Investigación y Desarrollo en Criotecnología de Alimentos (UNLP-CONICET), Facultad de Ciencias Exactas, UNLP, La Plata, Argentina*

Films based on thermoplastic corn starch (TPS) and talc nanoparticles were developed by melt mixing and thermo-compression. Films structure, optical and barrier properties, as well as thermal stability and water sorption behavior were studied. TPS structure resulted homogeneous and smooth. Talc laminar morphology and thermo-compression induced particle preferential orientation within the matrix. Good particle distribution and talc-TPS adhesion were evidenced. Nanometric thickness of mineral particles allowed obtaining translucent composite films, without significant color variation of TPS films. Talc addition at concentrations higher than 3% w/w led to an improvement on TPS barrier properties against water vapor and oxygen. It was also demonstrated that talc decreased water uptake of TPS films exposed to ambient conditions with relative humidity higher than 40%. In conclusion, films based on TPS and talc nanoparticles could be an alternative to develop biodegradable packages for food products with suitable final properties. POLYM. COMPOS., 00:000–000, 2016. © 2016 Society of Plastics Engineers

INTRODUCTION

Materials research and development from biodegradable and renewable raw inputs are in ongoing growth to supplement the use of petroleum-based polymers. In this sense, starch is a promising alternative mainly due to its world wide availability, biodegradable character, low cost, and functionality. Several authors studied the feasibility of using starches from different botanical sources to develop bio-based materials, such as films and coatings, with different final and functional properties [1–8]. Even though native starch is not considered a thermoplastic material, its processing under high temperature and shear stress, in presence of plasticizers, allows converting this biopolymer into thermoplastic starch (TPS) [9]. This is considered an advantage from the industrial point of view, since starch can be processed with the current technology designed for synthetic polymers [10]. This feature allows obtaining thermoplastic starch, without substantial financial investment by the processing industry. Despite the aforementioned advantages, TPS-based materials present poor mechanical properties and notable moisture absorption, conditioning their industrial and commercial applications. An option to overcome this limitation is to incorporate natural fillers or mineral particles within starch matrix, in order to enhance their final properties [11]. Thus, laminar morphology constituted by several stacked platelets, as well as, nanometric thickness and high aspect ratio (particle diameter/thickness $\approx$ 20:1) of talc particles make them a good alternative to reinforce several polymeric matrixes [12]. Besides, due to platelets are kept stacked by weak van der Waals forces, it could be possible the talc particles delamination during their processing with TPS, favoring the reinforcing effect of the polymeric matrix.

A promising application of TPS films is their use for food packaging. Thus, the design of packages should assure that product integral quality taking into account that mechanical, optical, and barrier properties of films would be the optimal ones for certain applications. Concerning to optical properties, mainly color and transparency, are relevant issues since they condition consumer acceptability of packed products. On the other hand, UV-vis absorption capacity of TPS films targets possible applications of these materials as radiation blockers for products susceptible to UV-oxidative rancidity or to develop packages that allow ulterior UV-sanitization of packed food [13]. Moreover, packages barrier properties play an important role controlling gases exchange, mainly

Correspondence to: Luciana A. Castillo; e-mail: lcastillo@plapiqui.edu.ar
DOI 10.1002/pc.24073
Published online in Wiley Online Library (wileyonlinelibrary.com).

water vapor and oxygen. These properties condition both organoleptic characteristics and microbial quality of the packed food. Another packages requirement is related to their water sorption behavior under several ambient conditions. Concerning to this, the study of films behavior exposed to different temperatures and relative humidities led to predict future industrial applications of these materials. In the same way, study of films thermal degradation gives information about the optimal processing conditions which warrantee the package integrity during product storage and transport.

The aim of this work was to process composites based on thermoplastic corn starch and talc nanoparticles by melt-mixing and thermo-compression. Processing conditions were optimized in order to tailor films with proper functional properties for food packaging applications. Thus, composites structure, optical, and barrier properties, as well as, their thermal stability and water sorption behavior were analyzed.

MATERIALS AND METHODS

Materials

Native corn starch was provided by Misky-Arcor (Tucumán, Argentina). Talc sample was supplied by Dolomita SAIC (Argentina). This mineral comes from an Australian ore, having a purity degree of 98% w/w. This is a platy talc sample conforming by particles with nanometric mean thickness of 79 nm, organized in laminar concentric domains like an "onion" structure [14, 15]. Besides, this talc has a microcrystalline morphology, where small platelets are stacked up heterogeneously. Glycerol was used as plasticizer.

Thermoplastic Starch Mixtures

Mixtures of starch, glycerol (30% w/w, starch basis), distilled water (45% w/w, starch basis), and talc (0, 1, 3, and 5% w/w, TPS basis) were prepared. Mixtures were processed in a Brabender Plastograph at 140°C and 50 rpm for 15 min. Torque–time curves were recorded by WinMix software and maximum torque as well as plasticization energy were determined following the procedure reported by Córdoba et al. [16].

Films Preparation

Thermoplastic starch films were obtained by thermocompression using a hydraulic press, following the processing conditions reported in a previous work [13]. Mixtures were conditioned at 25°C and 60% relative humidity (RH) and films were prepared at 140°C and 150 kg cm^{-2} during 6 min.

Films Microstructural Characterization

This study was carried out by scanning electron microscopy (SEM) in a JEOL JSM-35 CF electron microscope with a secondary electron detector, using an accelerating voltage of 10 kV. Films were cryo-fractured by immersion in liquid nitrogen, mounted on bronze stubs, and coated with a gold layer.

Films Optical Properties

Transparency and Blocking Effect. Absorbance spectrum (200–800 nm) was recorded using a Shimadzu UV-160 spectrophotometer. Films were cut into rectangles and placed on the internal side of a quartz spectrophotometer cell. Film transparency was estimated by using ASTM D1746-97 method and according the procedure reported by Alvarado-González et al. [17]. Each sample was analyzed by triplicate.

Blocking effect of talc to UV transmission was calculated with Eq. *1*, proposed by Sanchez-García et al. [18].

$$\text{Blocking effect} = \frac{T_{\text{TPS}} - T_{\text{Nanocomposite}}}{m_t}, \qquad (1)$$

where T_{TPS} and $T_{\text{Nanocomposite}}$ refer to percent transmittance for TPS and nanocomposite films, respectively and m_t is talc percent respect to starch mass. Blocking effect was calculated at 300, 350, and 750 nm in UV-B, UV-A, and visible region, respectively [19].

Color Measurements. Films color measurements were performed using a Hunterlab UltraScan XE colorimeter in the reflectance mode. Color parameters L, a, and b were recorded according to the Hunter scale, in at least 10 randomly selected positions for each film sample. Standard values considered were those of white background ($L = 97.75$, $a = -0.49$, and $b = 1.96$).

Films Barrier Properties

Water vapor permeability (WVP) was determined according to ASTM F 1249-89 standard method using a Permatran-W® Model 3/33 (Mocon Inc.). Measurements were carried out in triplicate at 25°C and water vapor transmission rate (WVTR) was registered using a RH gradient of 50%. Film samples were placed in a diffusion cell, separating it into two chambers. The inner chamber is flushed with nitrogen carrier gas (0% RH) and the outer chamber contains the permeant (humidified nitrogen stream, 50% RH). Masked specimens with precut aluminum foil were used, leaving an uncovered film area of 5 cm^2. WVP was calculated using Eq. *2*.

 DOI 10.1002/pc

$$\mathrm{WVP}=\frac{l\ \mathrm{WVTR}}{\Delta p}, \tag{2}$$

where l corresponds to film thickness (m) and Δp is the partial pressure difference across the film (Pa).

Oxygen mass transfer rates were analyzed at 25°C using a Mocon OX-Tran2/20 (Mocon Inc.) based on the ASTM 3985 standard method. Measurements in triplicate were carried out at 25°C, using an exposed area of 10 cm^2 and gases relative humidity was controlled at 75%. All film samples were previously conditioned at 25°C and 60% RH for WVP and oxygen permeation assays.

Thermal Stability and Water Sorption Behavior

Thermal degradation was carried out in a thermogravimetric balance TA Instrument Discovery Series. Samples were heated from 30 to 700°C at 10°C/min, under nitrogen atmosphere. Curves of loss weight as function of temperature were recorded and the onset decomposition temperature of each component was obtained from first derivative curves.

A static gravimetric method was used to determine water sorption isotherms of films. Samples (10 × 10 mm) were conditioned placing them inside a desiccator with $CaCl_2$ up to constant weight. Then, samples were placed inside nine vessels, with different water activities (a_w) from 0.1 to 0.98. Each relative humidity was reached from aqueous solutions with several glycerol concentrations. Samples were kept at 20°C up to equilibrium was attained. Moisture content of equilibrated samples was determined by Karl Fisher method, described by Skoog et al. [20]. Water sorption isotherms were built from experimental data, plotting humidity content at equilibrium as function of water activity. Experiences were carried at least by triplicate.

The Guggenheim–Anderson–de Boer (GAB) model was used to represent the experimental equilibrium data. GAB isotherm model can be expressed as follows:

$$X=\frac{m_0\ K\ C\ a_w}{(1-K\ a_w)(1-K\ a_w+C\ K\ a_w)}, \tag{3}$$

where X is the equilibrium moisture content at a water activity (a_w), m_0 is the water content of the monolayer value (g water/g solids) and C and K are GAB constants. The m_0 parameter was determined by nonlinear regression (Maple 14.00).

Statistical Analysis

Analysis of variance (ANOVA) was used to compare mean differences of sample properties. Besides, comparison of mean values was performed by Fisher's least significant difference test conducted at a significance level $p = 0.05$.

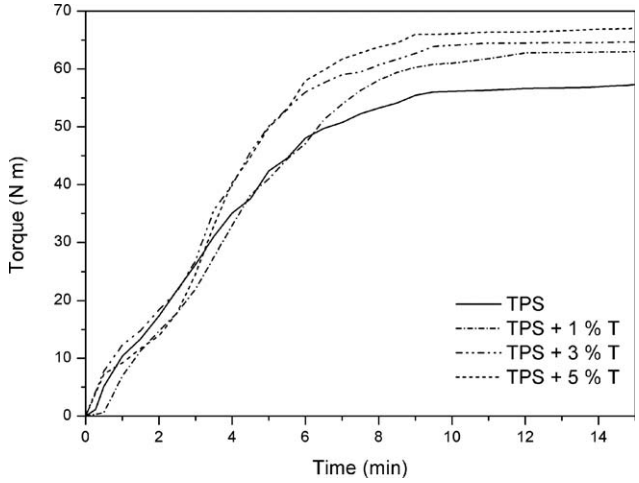

FIG. 1. Torque–time curves of composites based on TPS with different concentrations of talc nanoparticles (0, 1, 3, and 5% w/w).

RESULTS AND DISCUSSION

Composites Processing

Thermal processing of starch-based materials is more challenging than the corresponding to synthetic polymers. Liu et al. [21] reported that multiple chemical and physical reactions are involved during starch processing (water diffusion, granule expansion, gelatinization, decomposition, melting, and crystallization). Starch processing with plasticizers, at high shear stress and temperature, allows this biopolymer converting into a thermoplastic material. Córdoba et al. [16] reported that amylose molecules are released from the starch granular structure during its plasticization [22, 23]. In this sense, the amount of amorphous and granular regions in molten thermoplastic starch is dependent on processing conditions. Torque–mixing time curves obtained during melt processing of the studied nanocomposites are shown in Fig. 1. For TPS and composites, torque increased to a maximum value, which then is constant along the mixing time. Sample behavior in transient flow evidences that flow is determined by TPS behavior. Initial torque increment could be attributed to weak starch intermolecular interaction by hydrogen bonds as well as granules swelling [24]. For all formulations, torque reached equilibrium at the same time due to starch homogenization. Even all curves matched at the first stage, particles contributed to increment the composite flow resistance when equilibrium torque is reached, being this increase dependent on talc concentration. Moreover, particles orientation during processing, favored by their laminar morphology, led to the torque stabilization of TPS–talc composites. As a consequence of this orientation, particles area opposed to the flow direction is their transverse section, i.e., corresponding to the lowest dimension [25]. Thus, this hypothesis could justify the low increment in torque values with talc concentration.

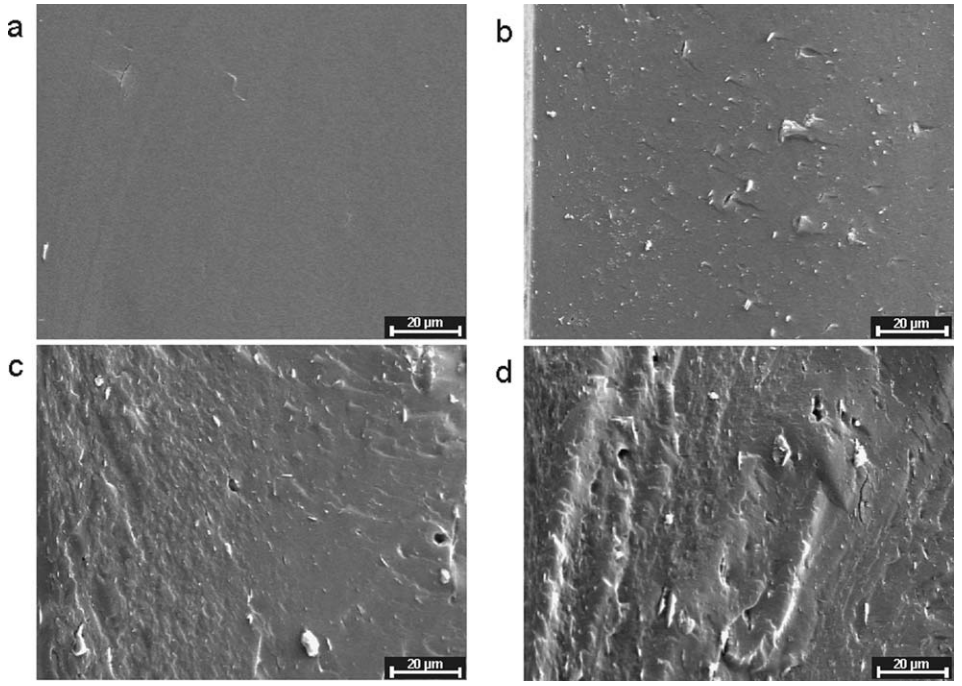

FIG. 2. SEM micrographs of TPS films with different concentrations of talc nanoparticles: (a) 0% w/w, (b) 1% w/w, (c) 3% w/w, and (d) 5% w/w.

Films Microstructural Characterization

In Fig. 2, SEM micrographs corresponding to the cross-sections of TPS composite films are presented. Film based on TPS evidenced a homogenous structure without the presence of starch granules, corroborating thermo-compression effectiveness (Fig. 2a). Films developed from TPS–talc composites presented a homogenous structure and talc particles were well distributed within the matrix (Fig. 2b–d). This observation is in accordance with the microstructure of composite based on starch and kaolinite reported by Mbey [19]. Similarly, Chung et al. [26] obtained starch–clays nanocomposites having homogeneous fracture surfaces and well particles distribution. When talc concentration increases, the presence of some aggregates is detected within the matrix since the small size of these particles favored the formation of aggregates during composites processing. Similar results were reported for starch–nanoclay composite films which evidenced continuous matrixes; however, their surfaces were less smooth than TPS ones [7]. On the other hand, an adequate adhesion of talc nanoparticles to TPS was observed, indicating a good compatibility between particles and matrix. Besides, talc laminar morphology allows particles alignment during thermo-compression and leads to a filler preferential orientation within the matrix. Similarly, Castillo et al. [15] reported a preferred orientation of talc particles within polypropylene-based composites, obtained by injection molding. These authors attributed this spatial distribution to particle plate-like structure and their motion in a viscous medium. During the compounding process, talc/molten polymer suspension flows and laminar particles align straight along the flow direction. Considering that particle orientation depends on the processing method, it is expected that blown extrusion would lead to a specific talc spatial alignment within the matrix. The increment of fracture surface irregularity of TPS films with an increase in particles concentration is attributed to talc addition, which increases TPS rigid phase (Fig. 2b–d).

Films Optical Properties

Since a feasible use of TPS films is to develop food packaging, the study of their optical properties is an important topic to be considered. Due to talc particles presence, composite films resulted less transparent than TPS ones (Fig. 3a). Nanocomposites films were homogenously translucent mainly due to the good particles distribution within starch matrix, corroborated by SEM, and the small particle size of talc. Transparency values corresponding to TPS films containing 5% w/w talc were similar to those of oriented polypropylene (1.67). On the other hand, these composite films resulted more opaque than those of low-density polyethylene (3.05) and polyvinyldichloride (4.58) [27].

From UV-vis spectra, particle blocking effect was also estimated at different wavelengths (Fig. 3b). When talc concentration increased from 1 to 3% w/w, a relevant decrease of light transmission at the three chosen wavelengths was observed. Mbey et al. [19] reported an analogous blocking effect by kaolinite presence in cassava

 DOI 10.1002/pc

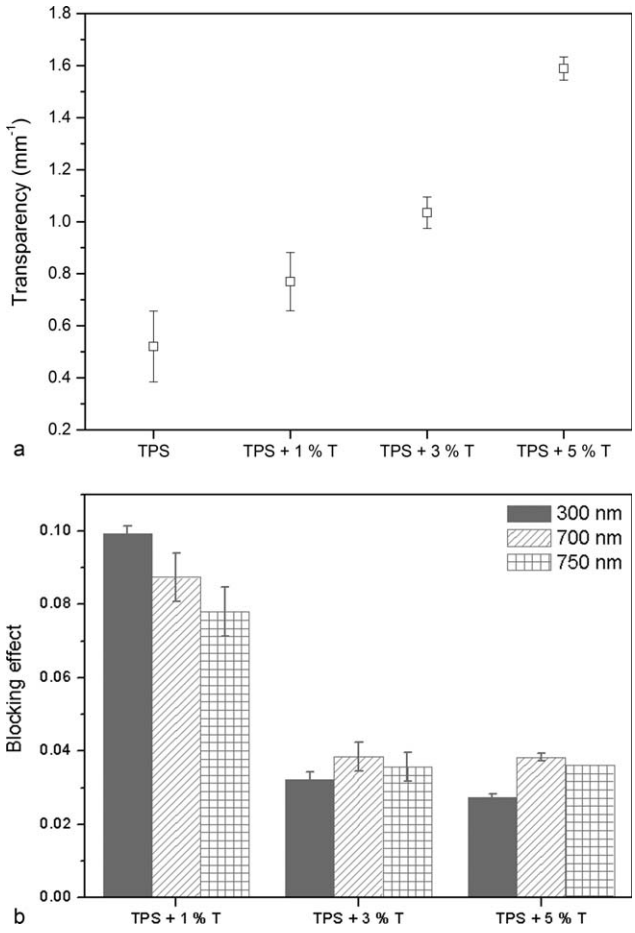

FIG. 3. (a) Transparency and (b) blocking effect of TPS films with different concentrations of talc nanoparticles (0, 1, 3, and 5% w/w).

starch films. Lower transparency could be also attributed to particles blocking effect against visible radiation.

Films Barrier Properties

Important issues in application field of these films as packaging materials are their barrier properties against different gases, especially water vapor and oxygen. Particularly, water vapor permeability should therefore be as low as possible in order to optimize the food package environment and potentially increase the shelf life of the food product [28]. Figure 4 shows WVP and oxygen permeability values of the developed materials. WVP corresponding to TPS films resulted significantly ($p < 0.05$) higher than those values of synthetic polymers: 1.3×10^{-12} g d^{-1} s^{-1} Pa^{-1} for polyvinylchloride, 9.3×10^{-13} g d^{-1} s^{-1} Pa^{-1} for low-density polyethylene, and 2.3×10^{-12} g d^{-1} s^{-1} Pa^{-1} for high density polyethylene [29, 30]. The fact that starch films present low water vapor barrier could be attributed to the hydrophilic nature of this polysaccharide and the swelling capacity of starch–glycerol network [31]. WVP of TPS films was not affected by the incorporation of talc at 1% w/w. However, particles concentration at 3 and 5% w/w reduced WVP of TPS in 31 and 54%, respectively. Likewise, other authors informed WVP reduction of starch films by addition of different mineral fillers [32–34]. In this sense, Slavutsky et al. [35] reported that the presence of montmorillonite particles increased barrier capacity against water vapor of corn starch films obtained by casting method. Besides, these authors stressed that this reduction in film permeability was related to the combined effect of the decrease in water solubility and the longer diffusive path that the penetrating molecules had to travel as the filler concentration increased.

On the other hand, TPS films had low oxygen permeation values in comparison to synthetic polymer ones (low and high density polyethylene shows values of 2,325 and 4,650 cm^3 mil m^{-2} d^{-1}, respectively). Similarly to WVP, composites containing 1% w/w talc presented the same oxygen permeation value than TPS films (Fig. 4). Meanwhile, talc addition at 3 and 5% w/w allowed 1.3 times increment of this barrier property, respect to TPS films. Talc layered structure is the responsible of WVP and oxygen permeation decrease of starch-based materials since particles increase the tortuous pathway for gases diffusion, hindering their flow through films matrix [36, 37].

Films Water Sorption Behavior and Thermal Stability

Water sorption isotherms provide information about materials hydrophilicity when they are exposed under different relative humidities. They represent the relationship between absorbed and desorbed water by materials and ambient water activity, at constant temperature, under equilibrium conditions [38]. Humidity sorption by starch-based materials is mainly attributed to biopolymer hydroxyl groups and water molecules interaction [39]. Figure 5 shows experimental data of equilibrium water content as a function of water activity for composite films. As it can be observed, films humidity content increased gradually up to $a_w = 0.7$–0.8; then this increment resulted exponential, being asymptotic when a_w tends to 1. This sigmoidal form is typical of starch and

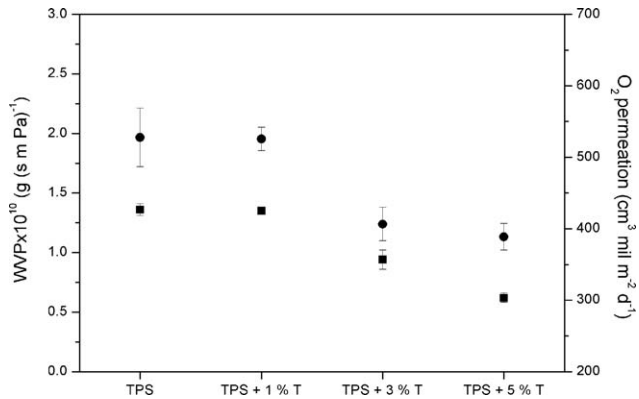

FIG. 4. WVP and oxygen permeation of TPS films with different concentrations of talc nanoparticles (0, 1, 3, and 5% w/w). Symbols: (■) WVP and (●) oxygen permeation.

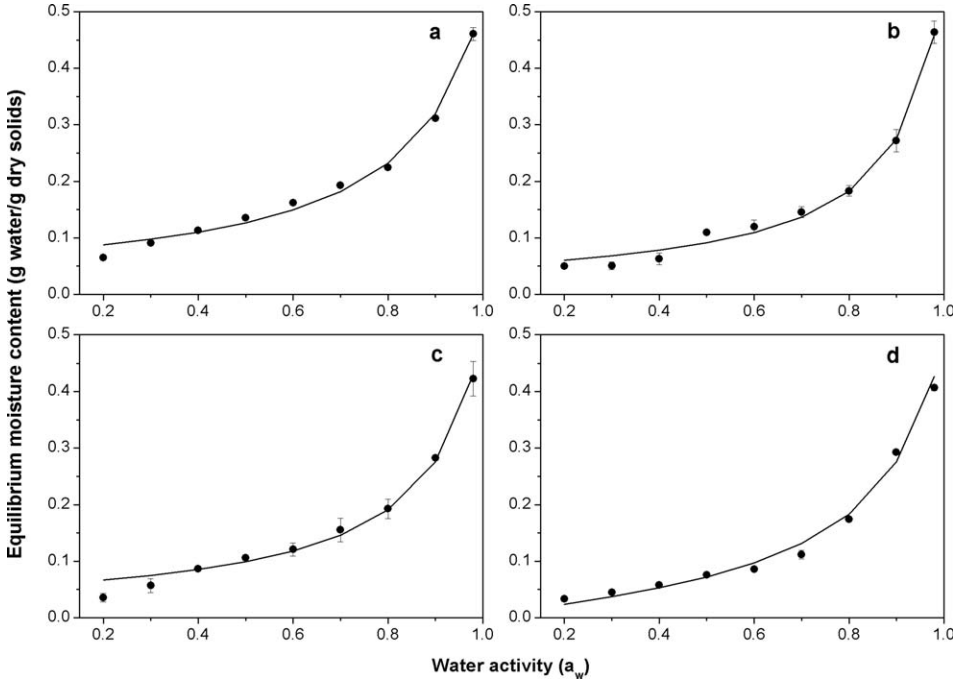

FIG. 5. Water sorption isotherms of TPS films with different concentrations of talc nanoparticles: (a) 0% w/w ($r^2 = 0.9863$, $m_0 = 0.072$), (b) 1% w/w ($r^2 = 0.9976$, $m_0 = 0.050$), (c) 3% w/w ($r^2 = 0.9953$, $m_0 = 0.055$), and (d) 5% w/w ($r^2 = 0.9971$, $m_0 = 0.069$).

protein rich products and it corresponds to Type II isotherms, according to BET classification. A significant increase ($p < 0.05$) of equilibrium water content from $a_w = 0.7$ could be attributed to a phenomenon called "water clustering," which was reported by other authors for starchy materials [33, 34, 36]. Even though films containing talc presented a similar behavior than TPS ones, particles incorporation reduced water sorption from $a_w = 0.4$. Similar results were reported by Masclaux et al. [40] for composites based on potato starch and montmorillonite (MMT). These authors reported that 7.5% w/w MMT modified water sorption behavior of starch matrix.

Decrease of TPS water sorption could be attributed to interactions between polymeric matrix and talc particles, causing a reduction of water capacity absorption in composite materials. According to Huang et al. [41], starch hydroxyl groups could interact with hydroxyl groups located at talc edge surfaces, conforming a compatible system which leads to an increased stability of composites at different environmental conditions. On the other hand, Tunc et al. [42] reported that humidity sensibility reduction of films based on hydrophilic biopolymers by mineral particles presence is due to specific interactions among mineral, glycerol and polymer. In this sense, Tang et al. [43] reported that composites nanostructure depends on compatibility and interactions among polymeric matrix, plasticizer and mineral sheets. According to these authors, strong polar interactions among starch, glycerol and mineral edge surface establish a competition mechanism which could explain the reduction of water sorption capacity of composites based on TPS by talc presence.

GAB model fitted adequately the experimental data for all studied formulations. This model was used for starch-based materials by several authors [44–47]. The m_0 parameter corresponds to the water content of the monolayer and obtained results are in accordance to values reported by other authors for starch films [46–49]. Despite talc incorporation reduced m_0 values of TPS films, it was not evidenced a net tendency with particles concentration. This observation could be mainly the consequence of two contributions. On one hand, the effect of talc hydrophobic character on m_0 parameter is diminished due to the major amount of particles are contained within the starch matrix, as it was detected by SEM (Fig. 2). On the other hand, the lack of tendency observed for m_0 with talc concentration may be related to the low filler contents used to develop starch-based composites. Moreover, Enrione et al. [44] reported that monolayer content of thermoplastic starch was not affected by the concentration and hydrophilic nature of nanoclay used as filler. They claimed that polymer matrix governs the sorption mechanism of TPS composites. Similar results were described by Masclaux et al. [40] for starch-based films reinforced with montmorillonite.

Thermal stability of materials based on starch is a relevant topic for both academic and industrial fields. In order to optimize starch processing, the understanding about degradation and thermal decomposition relationship is crucial [50]. Liu et al. [51] reported that the most important process associated to starch degradation are dehydration and decomposition. Figure 6 shows weight loss as a function of temperature, as well as, first

 DOI 10.1002/pc

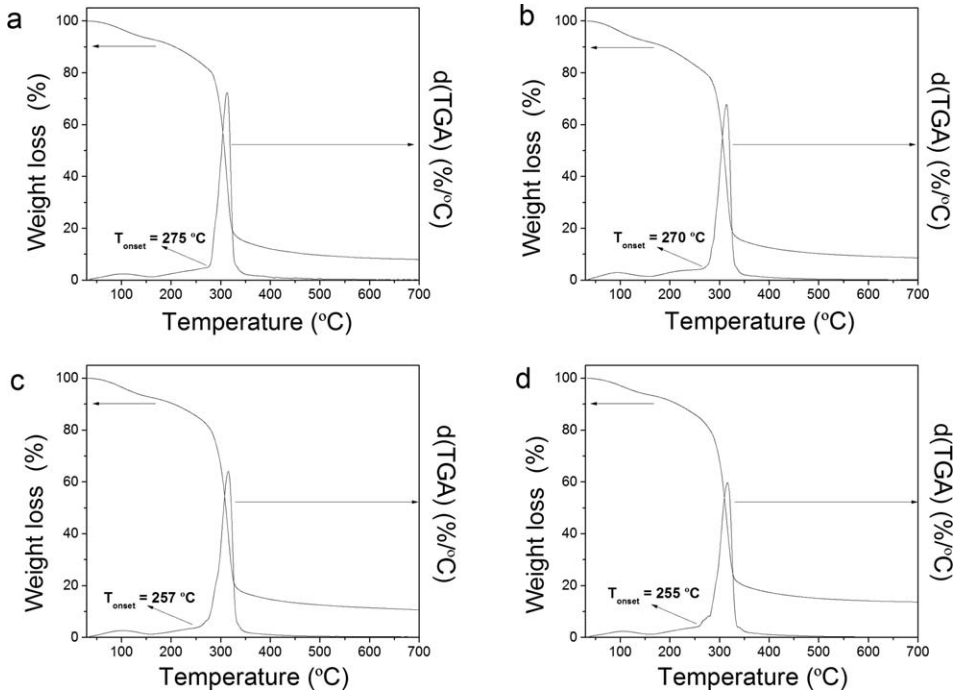

FIG. 6. TGA curves of TPS films with different concentrations of talc nanoparticles: (a) 0% w/w, (b) 1% w/w, (c) 3% w/w, and (d) 5% w/w.

derivative curves corresponding to the developed composite films. Along with temperature increase, several solid-state reactions and phase transitions take place, such as melting, evaporation and sublimation, as well as, chemical condensation, and decomposition [52]. As it can be observed, all curves presented a similar behavior, showing the occurrence of three weight loss steps, indicating that talc particles did not modify TGA pattern of TPS films. Each stage corresponds to a peak in the first derivative curve which represents a separate event in a particular temperature range. The first weight loss was associated to water desorption. Meanwhile, the second one could be attributed to glycerol lost, as it has been previously reported by other authors [50]. Finally, the most notable weight variation was related to the starch degradation. During this process, ether bonds and unsaturated structures are formed via thermal condensation between hydroxyl groups of starch chains, which eliminates water and other small molecules, and by dehydration of hydroxyl groups in the glucose ring [53]. Concerning to the influence of talc presence on TPS thermal stability, it could be observed a slight shift of starch onset degradation temperature toward lower values, detected in the first derivative curves. This tendency is in accordance with talc concentration increment in composite films.

CONCLUSIONS

TPS–talc films were obtained by melt mixing and thermo-compression. Talc influence on structure, optical and barrier properties, as well as, thermal stability and water sorption behavior of TPS films were studied. Even though flow during melt mixing seemed to be dominated by TPS behavior at the first processing stage, particles presence increased slightly composite flow resistance. Particle preferential orientation within starch matrix was evidenced due to talc laminar morphology, favored by thermo-compression process. In addition, an adequate particle adhesion to TPS was achieved due to the good compatibility between talc and starch matrix. Composite films were translucent, attributed to the nanometric thickness of mineral particles. However, a loss transparency of TPS films by talc presence was observed, associated to particles blocking effect against visible radiation. On the other hand, the incorporation of talc did not significantly affect color parameters of TPS films. Concerning to water vapor and oxygen permeability, addition of talc concentration higher than 3% w/w led to a notable reduction of these gases exchange through TPS films. From water sorption isotherms, it was concluded that talc decreased water uptake of TPS films from 40% RH. Talc presence induced a slight shift of starch onset degradation temperature toward lower values. Thus, the results derived from this study mainly those related to the increment of TPS water vapor barrier capacity as well as stability under high humidity conditions allows to propose the feasibility of using these composites films for food packaging as a new option of biodegradable materials based on natural products.

REFERENCES

1. L. Famá, S. Flores, L. Gerschenson, and S. Goyanes, *Carbohydr. Polym.*, **66**, 8 (2006).

2. M. A. García, A. Pinotti, M. N. Martino, and N. E. Zaritzky, Characterization of starch and composite edible films and coatings, in *Edible Films and Coatings for Food Applications*, M.E. Embuscado and K.C. Huber, Eds., Springer, New York, 69 (2009).
3. O. López, M.A. García, and N.E. Zaritzky, *Carbohydr. Polym.*, **73**, 573 (2008).
4. O. López, M.A. García, and N.E. Zaritzky, *Postharvest Rev.*, **6**, 1 (2010).
5. O. López, M.A. García, and N.E. Zaritzky, *J. Food Eng.*, **100**, 160 (2010).
6. O. López, C.J. Lecot, N.E. Zaritzky, and M.A. García, *J. Food Eng.*, **105**, 254 (2011).
7. C. De Melo, P. Garcia, M.V. Eiras Grossmann, F. Yamashita, L. DalÍAntônia, and S. Mali, *Braz. Arch. Biol. Technol.*, **54**, 1223 (2011).
8. C. Müller, J. Laurindo, and F. Yamashita, *Food Hydrocolloids*, **23**, 1328 (2009).
9. X. Ma, P. Chang, J. Yu, and M. Stumborg, *Carbohydr. Polym.*, **75**, 1 (2009).
10. D. Tapia Blácido, P. Sobral, and F. Menegalli, *J. Food Eng.*, **67**, 215 (2005).
11. V. Cyras, L. Manfredi, M. Ton-That, and A. Vazquez, *Carbohydr. Polym.*, **73**, 55 (2008).
12. L. Castillo, S. Barbosa, P. Maiza, and N. Capiati, *J. Mater. Sci.*, **46**, 2578 (2011).
13. L. Castillo, O. López, C. López, N. Zaritzky, M.A. García, S.E. Barbosa, and M.A. Villar, *Carbohydr. Polym.*, **95**, 664 (2013).
14. L. Castillo, S. Barbosa, and N. Capiati, *J. Appl. Polym. Sci.*, **126**, 1763 (2012).
15. L. Castillo, N. Capiati, and S. Barbosa, Mechanical properties of polypropylene/talc composites: role of the mineral morphology and particle surface modification, in *Polypropylene: Synthesis, Applications and Environmental Concerns*, L.P. Silva and E. Fernandes Barbosa, Eds., Nova Publishers Inc., New York, 145 (2013).
16. A. Córdoba, N. Cuéllar, M. González, and J. Medina, *Carbohydr. Polym.*, **73**, 409 (2008).
17. J. Alvarado-González, J. Chanona-Pérez, J. Welti-Chanes, G. Calderón-Domínguez, S. Arzate-Vázquez, S. Pacheco-Alcalá, V. Garibay-Febles, and G. Gutiérrez-López, *Rev. Mex. Ing. Qca.*, **11**, 193 (2012).
18. M. Sanchez-Garcia, L. Hilliou, and J. Lagaron, *J. Agric. Food Chem.*, **58**, 6884 (2010).
19. J. Mbey, S. Hoppe, and F. Thomas, *Carbohydr. Polym.*, **88**, 213 (2012).
20. D. Skoog, D. West, and F. Holler, *Química Analítica*, 6th Ed., McGraw-Hill, Mexico D.F. (1995).
21. H. Liu, F. Xie, L. Yu, L. Chen, and L. Li, *Prog. Polym. Sci.*, **34**, 1348 (2009).
22. W.S. Ratnayake and D.S. Jackson, *Carbohydr. Polym.*, **67**, 511 (2007).
23. A. Jimenez, M.J. Fabra, P. Talens, and A. Chiralt, *Food Bioprocess Technol.*, **5**, 2058 (2012).
24. X. Qiao, W. Jiang, and K. Sun, *Starch-Stärke*, **57**, 581 (2005).
25. C.H. Suh and J.L. White, *J. Non-Newtonian Fluid Mech.*, **62**, 175 (1996).
26. Y.-L. Chung, S. Ansari, L. Estevez, S. Hayrapetyan, E.P. Giannelis, and H.-M. Lai, *Carbohydr. Polym.*, **79**, 391 (2010).
27. S.F. Hosseini, M. Rezaei, M. Zandi, and F.F. Ghavi, *Food Chem.*, **136**, 1490 (2013).
28. Y. Zhang and J.H. Han, *JFS E: Food Eng. Phys. Prop.*, **71**, 273 (2006).
29. L. Massey, *Permeability Properties of Plastics and Elastomers—A Guide to Packaging and Barrier Materials*, 2nd Ed., Plastics Design Library, New York (2003).
30. M. Ghasemlou, N. Aliheidari, R. Fahmi, S. Shojaee-Aliabadi, B. Keshavarz, M.J. Cran, and R. Khaksar, *Carbohydr. Polym.*, **98**, 1117 (2013).
31. H. Pushpadass, A. Kumar, D. Jackson, R. Wehling, J. Dumais, and M. Hanna, *Starch-Stärke*, **61**, 256 (2009).
32. W. Gao, H. Dong, H. Hou, and H. Zhang, *Carbohydr. Polym.*, **88**, 321 (2012).
33. P. Kampeerapappun, D. Aht-ong, D. Pentrakoon, and K. Srikulkit, *Carbohydr. Polym.*, **67**, 155 (2007).
34. H. Park, X. Li, C. Jin, C. Park, W. Cho, and C. Ha, *Macromol. Mater. Eng.*, **287**, 553 (2002).
35. A.M. Slavutsky, M.A. Bertuzzi, M. Armada, M.G. García, and N.A. Ochoa, *Food Hydrocolloids*, **35**, 270 (2014).
36. X. Tang, S. Alavi, and T. Herald, *Cereal Chem.*, **85**, 433 (2008).
37. O. López, L. Castillo, M. García, M. Villar, and S. Barbosa, *Food Hydrocolloids*, **43**, 18 (2015).
38. A. Al-Muhtaseb, W. McMinn, and T. Magee, *J. Food Eng.*, **61**, 297 (2004).
39. R. Manek, O. Kunle, M. Emeje, P. Builders, G. Rao, G. Lopez, and W. Kolling, *Starch-Stärke*, **57**, 55 (2005).
40. C. Masclaux, F. Gouanvé, and E. Espuche, *J. Membr. Sci.*, **363**, 221 (2010).
41. M. Huang, J. Yu, and X. Ma, *Polymer*, **45**, 7017 (2004).
42. S. Tunc, H. Angellier, Y. Cahyana, P. Chalier, N. Gontard, and E. Gastaldi, *J. Membr. Sci.*, **289**, 159 (2007).
43. X. Tang and S. Alavi, *Carbohydr. Polym.*, **85**, 7 (2011).
44. J.I. Enrione, S.E. Hill, and J.R. Mitchell, *Starch-Stärke*, **59**, 1 (2007).
45. L. Godbillot, P. Dole, C. Joly, B. Rogé, and M. Mathlouthi, *Food Chem.*, **96**, 380 (2006).
46. S. Mali, L.S. Sakanaka, F. Yamashita, and M.V.E. Grossmann, *Carbohydr. Polym.*, **60**, 283 (2005).
47. C.M.O. Müller, F. Yamashita, and J.B. Laurindo, *Carbohydr. Polym.*, **72**, 82 (2008).
48. J.M. Krochta and R. Sothornvit, *J. Food Eng.*, **50**, 149 (2001).
49. C. Zeppa, F. Gouanvé, and E. Espuche, *J. Appl. Polym. Sci.*, **112**, 2044 (2009).
50. J. Mano, D. Koniarova, R. Reis, C. De Azure, and C. De Gualtar, *J. Mat. Sci. - Sci. Med.*, **14**, 127 (2003).
51. X. Liu, Y. Wang, L. Yu, Z. Tong, L. Chen, H. Liu, and X. Li, *Starch-Stärke*, **65**, 48 (2013).
52. K. Pielichowski and J. Njuguna, *Thermal Degradation of Polymeric Materials*, Rapra Technology Limited, Crewe, UK (2005).
53. R. Ruseckaite and A. Jiménez, *Polym. Degrad. Stab.*, **81**, 353 (2003).

 DOI 10.1002/pc